THE ASTROPHYSICAL JOURNAL, 475:803–811, 1997 February 1

THE SHELL OF RECURRENT NOVA T PYXIDIS: A MODEL BASED ON SHOCKS

MARCELLA CONTINI[1] AND DINA PRIALNIK[2]
Received 1996 April 2; accepted 1996 August 12

ABSTRACT

A model for the shell of the recurrent nova T Pyxidis is presented, consistent with the bulk of observational data on this object. Evolutionary calculations of thermonuclear runaways on the surface of an accreting white dwarf that simulate the observed outburst characteristics of this nova—recurrence time, rise time, time of decline, luminosity—provide the mass of the ejected shell, its composition, and the effective temperature and luminosity of the nova in quiescence (for a white dwarf mass of 1.25 $M_\odot$, a core temperature of 10^7 K, and an accretion rate of 10^{-7} $M_\odot$ yr^{-1}). These results are used as input parameters for the SUMA code, which simulates the physical conditions of an emitting gaseous cloud under the combined effects of photoionization and shocks. The shell model involves two emitting regions besides the central star (which is the main UV radiation source), both resulting from compressed gas behind a shock front. The shocks are assumed to be produced by the collision between two extended shells ejected at consecutive outbursts. As a result of the collision, a secondary blast wave propagates outward into the older ejecta, while a reflected (reverse) shock wave propagates back through the new ejecta. Applying the SUMA code to each zone, we find that different lines are emitted in the two zones, and combined, they account for the entire observed line spectrum. The absolute fluxes in different spectral ranges agree with those derived from observations, assuming a distance of $\sim$2 kpc. The derived abundances imply that mixing has taken place between the nova ejecta and interstellar material. Nevertheless, helium is overabundant and N/O is high. The model accounts for the observed structure of the nebula surrounding T Pyx, including the inner shell, the stagnant outer shell, and the extended faint region beyond it.

Subject headings: novae, cataclysmic variables — shock waves — stars: abundances — stars: individual: (T Pyxidis) — stars: mass loss — white dwarfs

1. INTRODUCTION

The recurrent nova (RN) T Pyxidis has had five recorded outbursts (in 1890, 1902, 1920, 1944, and 1966), all of which were very similar photometrically and were relatively slow to rise and decline (Warner 1995, and references therein). During the extent of the last outburst, several detailed observations were carried out by Catchpole (1969). We note, in particular, that different expansion velocities were derived from these spectroscopic observations, ranging from 300 km s^{-1} to 2000 km s^{-1}. Although these corresponded to various observation times, as many as three different velocity systems were found to be coexisting. The general shape of the light curve and the velocity range were found to agree well with observations of the previous outbursts (Payne-Gaposhkin 1957).

The most detailed spectrum of the T Pyx shell was provided by the observations of Williams (1982), carried out in 1980, i.e., in quiescence, 14 yr after the last outburst. The shell, $\sim$10″ in diameter, was then believed to represent the ejecta of the 1966 eruption (although a possible origin of the shell from the 1944 outburst could not be completely ruled out). Velocities deduced from spectroscopic observations carried out in 1981 (Williams 1983) were of the order of several hundred km s^{-1}.

The shell surrounding T Pyx was observed again about 5 yr later ($\sim$20 yr after the last eruption) by Shara et al. (1989). A puzzling feature of the shell emerged from the comparison of the 1980 and 1985 images, which showed that the $\sim$10″ diameter had barely grown in size during the 5 yr period. An expansion velocity of no more than $\sim$350 km s^{-1} was derived for the gas within the bright shell. This low expansion rate is in sharp contrast to the rapid expansion prior to this period, which must have occurred, if the shell was, indeed, generated by the 1966 outburst. The 1985 observations also revealed a ring $\sim$4″ in diameter and a faint, extended, diffuse envelope, almost 20″ in diameter. An alternative interpretation was therefore suggested: the ring closer to the star represents material ejected during the most recent outburst, in 1966 (Seitter 1986; Duerbeck 1987), while the distant shell is the ejecta of the 1944 outburst; the faint, extended envelope is the remnant of the 1920 (and perhaps earlier) eruptions. This, however, implies a very low expansion velocity for the 1966 ejecta, in apparent disagreement with the high ejection velocities observed at the 1966 outburst. Thus, the problem of the T Pyx nebula is still unsolved.

The ambiguity regarding the age of the shells and the multiple velocity systems render a direct estimate of the distance to T Pyx rather uncertain. However, as its spectrum is quite similar to that of classical novae (CNs), the absolute magnitude–time of decline relationship may be used to estimate the distance, which yields 1.9 kpc (Williams 1982). A different estimate, based on the strength of the interstellar Ca II K line (Catchpole 1969), yields 1 kpc. Taking into account the bulk of observational evidence, Webbink et al. (1987) conclude that the distance to T Pyx could be anywhere between 1 and 4.5 kpc. A more recent estimate, based on reddening values determined from the λ2175 line, yields 3.5 kpc (Selvelli, Gilmozzi, & Cassatella 1995).

[1] School of Physics and Astronomy, Raymond and Beverly Sackler Faculty of Exact Sciences, Tel Aviv University, Ramat Aviv 69978, Israel.

[2] Department of Geophysics and Planetary Sciences, Raymond and Beverly Sackler Faculty of Exact Sciences, Tel Aviv University, Ramat Aviv 69978, Israel.

Over the years, fluxes were measured in different spectral ranges (Seaquist & Taylor 1990; Skody et al. 1991; Harrison, Johnson, & Spyromilio 1993; Weight et al. 1994; Harrison & Gehrz 1994; Skody 1994; Bruch & Engel 1994). The UV emission of this nova has been monitored by *IUE* between 1986 and late 1994 (Selvelli et al. 1995). The continuum energy distribution is found to be remarkably constant, while the emission lines exhibit substantial intensity changes on timescales of the order of a few hours. Based on the *IUE* observations, Selvelli et al. derive a UV continuum luminosity of 90 $L_\odot$ and infer a lower limit of $2 \times 10^{-8}\ M_\odot$ yr^{-1} for the mass accretion rate (assuming the UV flux is emitted by the central source and adopting a distance of 3.5 kpc).

The purpose of this paper is to present a consistent model for RN T Pyx. Assuming the eruptions are triggered by thermonuclear runaways on the surface of an accreting white dwarf (WD) (see Starrfield, Sparks, & Truran 1985; Webbink et al. 1987; Kato 1990; Prialnik & Kovetz 1995), as are classical nova eruptions, we choose first a set of initial parameters for evolutionary calculations that reproduce successfully (most of) the observed general characteristics of the nova (Prialnik & Kovetz 1995): recurrence time, time of decline, and outburst amplitude. The evolution model provides additional information that is more difficult (or impossible) to derive from observations, such as the mass of the ejected shell and its composition and the effective temperature and (bolometric) luminosity of the nova at all times. This information, together with observationally derived characteristics of the shell, is then used as input data for a code that simulates the physical conditions of an emitting gaseous cloud under the combined effects of photoionization and shocks (the code known as SUMA, developed by Contini & Aldrovandi 1983; see Viegas & Contini 1994, and references therein).

The constant radius of the shell around T Pyx could represent a standing shock caused by the encounter of the ejecta with circumstellar gas of earlier eruptions. Thus, we consider the possibility of shocks in the context of an elaborate model, although this possibility has been dismissed on the basis of the absence of [O I] λ6300 and [S II] $\lambda\lambda$6717, 6734 emission lines in Williams's (1982) spectra (Shara et al. 1989). The physical conditions required to reproduce the observed line intensity ratios, although not uniquely determined, will provide a full and consistent picture of this nova and its ejecta.

In § 2 we present briefly an evolutionary model for this RN; in § 3 we describe the general structure of the T Pyx shell, on which the ionization models are based; in § 4 we show results of model calculations for the shell due to the combined effect of photoionization and shocks; and a discussion follows in § 5.

2. AN EVOLUTIONARY MODEL FOR T PYX

Among the grid of evolutionary models of novae carried out by Prialnik & Kovetz (1995), the last one that best fits the characteristics of T Pyx is obtained for a 1.25 $M_\odot$ cold white dwarf (core temperature of 10^7 K), accreting at a rate of $10^{-7}\ M_\odot\ yr^{-1}$. The outburst recurrence period for this parameter combination is $\sim$19 yr, equal to the *average* period of time elapsed between the observed outbursts. The 1966 outburst required 32 days to reach maximum light. This indicates a very slow expansion of the envelope until the time of ejection. In the model, the expansion phase prior to mass ejection lasted for 26 days, a very unusual behavior, when compared to the very rapid rise of modeled CNs. The agreement with observations is all the more significant. The duration of the mass loss phase t_{m-1}, which is a close lower limit to the time of decline by 3 mag t_3, is 65 days, the observed t_3 being 88 days. The time of decline of the bolometric luminosity is close to 9 months. According to Catchpole's (1969) observations, 346 days after maximum the star appeared to be at minimum brightness, which imposes an upper limit of less (perhaps much less) than 1 year for the time of decline of the bolometric luminosity. A comparison between observations and calculations is given in Table 1.

TABLE 1

NOVA CHARACTERISTICS

Characteristic	Observations	Model
P_{rec} (yr)	19	19
t_{rise} (days)	32	26
t_3/t_{m-1} (days)	88	$\gtrsim$65
t_{3bol} (days)	<346	$\sim$360
M_v/M_{bol}	−6.5	−6.5
v (km s^{-1})	300–2000	300–500
m_{ej} ($M_\odot$)	...	1.6(−6)
[He/H]	...	0.156
[C/H]	...	1.9(−4)
[N/H]	...	2.7(−3)
[O/H]	...	2.6(−4)

The evolution of the bolometric luminosity through the outburst, mass-loss, and decline phases is given in Figure 1, together with the evolution of the nuclear luminosity. A maximum absolute magnitude of −6.5 was deduced for the 1966 outburst of this nova, based on the time of decline–maximum brightness relationship for CNs (which also implies a distance of $\sim$2 kpc to this nova), in excellent

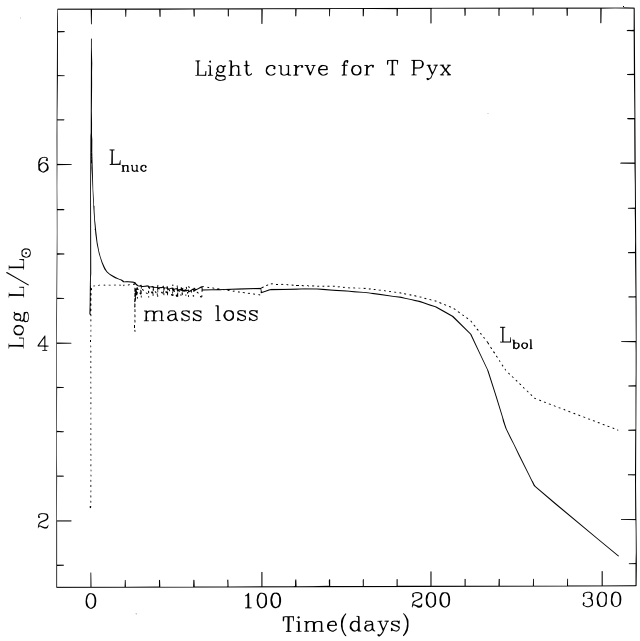

FIG. 1.—The evolution of the bolometric luminosity and of the nuclear luminosity during a typical outburst for a model calculated with the following parameters: $M_{WD} = 1.25\ M_\odot$, $T_{WD} = 10^7$ K, and $\dot{M} = 10^{-7}\ M_\odot$ yr^{-1}, which simulates the observed characteristics of the RN T Pyx.

agreement with bolometric magnitude derived from the calculations. The luminosity at minimum (the accretion luminosity, essentially) is $L \approx 120\ L_{\odot}$, and the effective temperature is $T_e \approx 2.7 \times 10^5$ K. The WD's radius is $R_{\rm WD} = 3.5 \times 10^8$ cm. The values of L and T_e should be considered as averages, in case of a variable accretion rate. According to the ratio He II/Hβ, which is a measure of the temperature of the hot source, the stellar temperature of the primary component of T Pyx (at minimum) is, indeed, estimated to be on the order of 10^5 K (Duerbeck & Seitter 1990), similar to that of other two RNs, U Sco and V394 CrA.

The mass ejected in each outburst is $m_{\rm ej} - 1.6 \times 10^{-6}\ M_{\odot}$, considerably lower than that inferred by Kato (1990), but well above the lower limit deduced by Webbink et al. (1987) to account for the Hβ flux. The average expansion velocity of the ejecta $v_{\rm av}$ is 350 km s^{-1}. Typical of CN outbursts, the velocity of the ejected mass is not unique. The range of expansion velocities obtained is from 500 km s^{-1} to 300 km s^{-1}, the highest velocity corresponding to the early stage of mass loss. The general trend is a gradual decrease of the velocity, as mass loss continues. We note, however, that the method of mass-loss calculation, based on the optically thick wind mechanism, is apt to underestimate the expansion velocities at the very onset of an outburst, when material may be accelerated by a shock (Prialnik 1986), propagating outward from the base of the nova envelope. The calculated minimal velocity is thus more reliable than the maximal one. The minimal velocity obtained is in very good agreement with the observations. We should mention that the kinetic energy of the ejecta constitutes a very small fraction of the outburst energy supplied by the nuclear reactions: while the energy required to expel the ejecta from the WD's gravitational potential well is $\sim 1.2 \times 10^{45}$ ergs, and the integrated luminosity over one cycle is $\sim 3 \times 10^{45}$ ergs, the calculated kinetic energy is only $\sim 2 \times 10^{42}$ ergs. Even if the outburst velocity were 2000 km s^{-1} for the entire ejected mass, the associated kinetic energy would have amounted to less than 10^{44} ergs, and hence it would not have required a significantly stronger outburst than that of the present model.

The abundances of the ejecta (by number, relative to hydrogen) are given in Table 1. The heavy element content (Z) is only slightly above solar; helium, however, is enhanced with respect to hydrogen. A characteristic feature of novae is the high N/O ratio obtained. The predicted abundances of the ejecta constitute a crucial input parameter for the following emission model that will have to match the observed line intensity ratios of the T Pyx shell(s).

3. THE STRUCTURE OF THE T PYX SHELL

The main objective of this paper is to model the emission of the ejected shell of T Pyx by reproducing the line spectrum using the SUMA code, which simulates the physical conditions of an emitting gaseous cloud under the coupled effects of shocks and photoionization. As noted by Williams (1982), the spectrum is too poor in number of lines to constrain the input parameters of a model to a unique set. The constraints imposed by the evolutionary characteristics of the system will help to rule out (at least) some of the models that match the line spectrum. We aim at a model that is compatible with the bulk of observational data.

The shell model is based on the following general scenario. As the recurrence period is short, and the range of expansion velocities of the ejecta is quite wide, it is inevitable that the shell expelled in any outburst will, eventually, encounter the shell expelled in the preceding one. Thus, after an initial stage of free expansion in a dilute interstellar medium (ISM), the ejecta will interact with a medium of higher density, created by the expanding shell of the earlier outburst. As a result, a spherically symmetric blast wave will propagate outward into this medium, while a reverse strong shock will propagate back into the ejecta (see Chevalier 1982). The situation is similar to that of an expanding supernova remnant, which has been studied intensively (see Ostriker & McKee 1988, and references therein). The initially high velocity of the blast wave will produce high densities and temperatures behind the shock front, and hence hard X-ray emission would be expected. However, as it expands and sweeps up additional material, the blast wave decelerates. Eventually, the X-ray emission will subside and the ionized region behind the decelerated shock front will become visible in Hα. When the amount of material swept up by the shock is of the order of the ejected material, assuming a uniform, homogeneous ambient medium, the standard self-similar Sedov-Taylor solution applies. This solution depends on two parameters: the energy E and the ambient density ρ_0. The blast wave radius as a function of time is given by

$$R_s(t) = \xi (E/\rho_0)^{1/5} t^{2/5}\ , \tag{1}$$

where the coefficient $\xi = 1.17$, while the shock velocity varies as $R_s^{-3/2}$,

$$V_s = \tfrac{2}{5} \xi^{5/2} (E/\rho_0)^{1/2} R_s^{3/2} \tag{2}$$

(Sedov 1959). At the same time, the reverse shock will proceed toward the center and will, eventually, dissipate when the entire ejecta will have passed through it. Soon enough a new outburst will occur, and the process will repeat itself.

It is plausible that the lumpy nature of the extended T Pyx shell is a result of turbulence caused by the collision between two consecutively ejected shells (Gull 1973, 1975). Each shell is swept by two shock waves: first, the reflected wave, generated at the outer boundary of the shell by the collision with earlier ejecta, propagates inward; later on, the blast wave, generated at its inner boundary by the collision with later ejecta, propagates outward.

We suggest the following configuration at the time of the 1980 and 1985 observations: the (almost) stagnant bright shell 10″ in diameter represents the ionized region behind the decelerated blast wave of the 1966 outburst, propagating through the extended ejecta of the earlier (1944) outburst. As the deceleration takes effect when the material swept up by the blast wave is comparable to that of the ejecta, the shock front must have advanced well into the 1944 ejected shell. The faint nebula observed beyond the bright 10″ shell could be the rest of the 1944 ejecta, downstream of the shock front. The ring (shell) close to the central star is produced by the reverse shock, propagating back into the 1966 ejecta. In this case, ionization is caused both by the shock and by the radiation of the hot central star.

In order to test the plausibility of this scenario, we make some rough estimates of the physical characteristics involved, assuming consecutive outbursts to be very similar, as indicated both by observations and by evolutionary calculations. The distance estimate obtained from the absolute

magnitude–time of decline relationship, roughly $d \sim 2$ kpc, which is compatible with our evolutionary model of this nova, would place the observed outer shell of 10″ diameter at $\sim 1.4 \times 10^{17}$ cm from the central star. This would be the approximate radius of the blast wave R_s at the time of observation in 1980; that is, 14 yr after outburst. Let $P_{\rm rec}$ be the recurrence period (~ 19 yr, as dictated by observations and model calculations), let $v_{\rm min}$ be the minimum ejection velocity (~ 300 km s^{-1}), and let $v_{\rm max}$ be the (less certain) maximum velocity. Let R_c be the distance from the central star at which the outer edge of a newly ejected shell should encounter the inner boundary of the shell ejected in the previous outburst, and let t_c be the time of collision (measured from the latest outburst). Then

$$R_c \approx (P_{\rm rec} + t_c)v_{\rm min} \approx t_c\, v_{\rm max} ,$$

which yields

$$R_c \approx \frac{P_{\rm rec}\, v_{\rm min}}{1 - v_{\rm min}/v_{\rm max}} \approx \alpha P_{\rm rec}\, v_{\rm min} , \tag{3}$$

and

$$t_c \approx \frac{P_{\rm rec}\, v_{\rm min}}{v_{\rm max} - v_{\rm min}} \approx (\alpha - 1)P_{\rm rec} , \tag{4}$$

where

$$\alpha = \frac{1}{1 - v_{\rm min}/v_{\rm max}} \quad 1 < \alpha < 2 . \tag{5}$$

If $v_{\rm max} \sim 2000$ km s^{-1}, t_c would be ~ 4 yr and $R_c \approx 2 \times 10^{16}$ cm; a lower maximal velocity would imply a later collision and larger R_c. (If X-ray observations were carried out at the time of collision between the 1966 and 1944 shells [say, around 1970], they should have detected strong X-ray emission due to the rapidly outward moving blast wave.) The average density of the medium into which the blast wave propagates, ρ_0, may be estimated by assuming the shock has swept a considerable fraction of the 1944 shell, as well as ambient ISM material, by the time of observation and has thus been decelerated:

$$\rho_0 \approx \frac{3m_{\rm ej}(1 + \eta)}{4\pi(R_s^3 - R_c^3)} \approx (1 + \eta)10^{-24}\ {\rm g\ cm^{-3}} , \tag{6}$$

where $\eta = m_{\rm ISM}/m_{\rm ej}$ ($m_{\rm ISM}$ being the ISM mass mixed with the ejecta), to be determined by the shell model. Substituting these estimates in equation (1), we obtain the energy of the shock $E \approx 10^{43}$ ergs, which is compatible with the estimated kinetic energy of the ejecta (see § 2). Substituting, in turn, E, ρ_0, and R_s in equation (2), we obtain $V_s \sim 350$ km s^{-1}, in excellent agreement with the observations, if the outer shell represents a standing shock front. We should, perhaps, mention that factor of 2 errors in the assumed parameters would not alter the general picture.

4. THE SPECTRUM OF T PYX

With this model in mind, we attempt now to reproduce the observed emission-line spectrum by means of the SUMA code. As there are two emitting zones—one close to the star, where ionization is caused by the combined effect of the reverse shock and the stellar radiation, and another, further away, produced by the outgoing shock (the blast wave)—we obtain two different contributions to the spectrum. The spectrum emitted by the inner shell of ionized gas (computed by a composite model) is dominated by radiation rather than by the shock (it will be denoted RD hereafter), while the gas of the distant outer shell yields a pure shock-dominated spectrum (and will be denoted SD hereafter). Their relative weights will have to be determined.

4.1. *Constraints Imposed on the Model Parameters*

The parameters of the model are the gas density and composition, the shock velocity and the magnetic field in each zone, as well as the ionizing photon flux and the ionization parameter for the RD zone. The number of *free* parameters is, however, reduced significantly by the observed characteristics of the shell and by characteristics derived from the evolutionary calculations. Thus, as a fixed input parameter we assume an effective temperature $T_* = 2.5 \times 10^5$ K for the hot star, implying an ionizing photon flux $F_\nu = 2 \times 10^{27}$ cm^{-2} s^{-1}. This flux is related to the ionization parameter and the gas (number) density $n_{0,r}$ in the RD zone by

$$F_\nu\left(\frac{R_{\rm WD}}{R_r}\right)^2 = Un_{0,r}c , \tag{7}$$

where $R_{\rm WD}$ is known from the modeled nova outburst and R_r, the distance of the ionized shell from the central star, should be in the region of the inner observed shell. The distance of the outer shock front from the central star R_s is not a parameter of the ionization model (except that it should be sufficiently large for the radiation source to be negligible there); nevertheless, it serves to constrain other parameters of the model. For example, the (undisturbed) densities of the two zones, each produced by the ejecta of an outburst (mixed with ISM material), should be related roughly as the ratio of their volumes:

$$n_{0,r}/n_{0,s} \approx [(R_s/R_r)^3 - 1] . \tag{8}$$

An estimate of the average density in the outer shell is provided by equation (6). However, as the shell appears to be extremely clumpy (Shara et al. 1989), the density of material within clumps—responsible for the emission—is higher, implying a small filling factor f. Clumpiness is a characteristic feature of nova shells: for example, a filling factor of 1.3×10^{-3} was found by Andrea et al. (1991) for Nova PW Vul, and a value as low as 1.7×10^{-5} was deduced by Snijders et al. (1984) for the ejecta of Nova Aquilae 1982. In conclusion, the densities may be obtained in terms of the parameters η and f (or vice versa), assuming the latter have similar values in the two zones.

The parameter η, together with the calculated abundances of the ejecta, determine (or should be compatible with) the abundances of the shell relative to hydrogen that produce the line spectrum. Assuming solar composition for the ISM material, we have

$$\frac{\rm He}{\rm H} = \frac{({\rm He/H})_{\rm ej} + \eta {\rm H}_\odot/{\rm H}_{\rm ej}({\rm He/H})_\odot}{1 + \eta {\rm H}_\odot/{\rm H}_{\rm ej}} , \tag{9}$$

for the relative abundance of helium in the shell, and similar expressions for the other elements.

According to equation (2), if the outer shell represents a standing shock front, the shock velocity should be, as estimated earlier, ~ 350 km s^{-1}. The velocity of the reverse shock relative to the gas should be higher, both because the

expansion velocity of the gas should be higher and because the shock moves opposite to the gas. Thus, we are left with 5 essentially adjustable parameters (e.g., $\eta, f, V_{s,r}$ and the magnetic field strength in each zone), the others having to be compatible with them, if the model is to be self-consistent.

The results of the SUMA code calculations are line intensity ratios, integrated fluxes in different spectral ranges, and the spectral energy distribution (SED) of the continuum. The procedure is to vary the values of the adjustable parameters—which are constrained, also, by the physical characteristics of the system, but to a lesser extent—until an optimal fit to observed line intensity ratios is achieved. If a good fit is obtained, we test the plausibility of the model by comparing the resulting fluxes with those derived from observations, within the framework of the entire model. The relative weight w of the two contributions should be compatible with the ratio of their effective surfaces, as follows:

$$F_{\mathrm{H}\beta,\mathrm{obs}}\, d^2 = F_{\mathrm{H}\beta,r} R_r^2 f^{2/3} + F_{\mathrm{H}\beta,s} R_s^2 f^{2/3} = R_r^2 f^{2/3}(F_{\mathrm{H}\beta,r} + wF_{\mathrm{H}\beta,s}) . \quad (10)$$

In order to check how stringent our determination of the adjustable parameters is, we have run the program with different values and tested the effect on the line intensity ratios.

4.2. *General Characteristics of the Spectrum*

The observed spectrum is characterized by the absence of [O I] and [S II] lines, while the ratios [N II]/Hβ and [O II]/Hβ, as well as [O III]/Hβ, are rather high. The line ratio He II/He I is very high ($\gg 1$) due to radiation from the hot component. The low [O III] λ5007/[O III] λ4363 indicates that the emitting gas has a temperature in excess of 10^5 K and/or a density in excess of 10^5 cm^{-3}. However, if the gas is heated and ionized by pure radiation, it cannot reach such high temperatures, and the relatively high [O II]/Hβ ratio precludes densities higher than 10^4 cm^{-3}, because of the low critical density for collisional de-excitation of O^+ (less than 3×10^3 cm^{-3}). This apparent difficulty can be overcome by invoking shocks, which are easily capable of heating the gas to temperatures higher than 5×10^4 K. Their presence is also indicated by the FWHM of the lines, which implies velocities exceeding 300 km s^{-1}. As we have seen in the previous section, shocks are a natural consequence of the system's evolution. Finally, we note that the strength of the He II λ4686 emission line in the observed spectrum may be indicative of a relatively strong magnetic field (see Williams 1989).

TABLE 2

MODEL PARAMETERS

Parameter	RD Zone	SD Zone
V_s (km s^{-1}).....	550	300
n_0 (cm^{-3})	3000	200
B_0 (G)	1.(−3)	1.(−4)
T_* (K)	2.5(5)	...
U	1.(−3)	...
D (cm)	2.6(16)	...
[He/H]	0.11	0.11
[C/H]	3.0(−4)	3.0(−4)
[N/H].....	6.4(−4)	6.4(−4)
[O/H].....	2.3(−4)	2.3(−4)
[Ne/H]	8.3(−5)	8.3(−5)
[Mg/H]	2.6(−5)	2.6(−5)
[S/H]	5.1(−6)	5.1(−6)
[Si/H].....	3.3(−5)	3.3(−5)
[A/H]	6.3(−6)	6.3(−6)
[Fe/H]	4.0(−5)	4.0(−5)

The best fit to the observed line spectrum is obtained with an ionization parameter $U = 0.001$, shock velocities (relative to the gas) $V_s = 550$ km s^{-1} and 300 km s^{-1} for the reverse and outward shocks, respectively, and gas preshock densities by number $n_0 = 3000$ cm^{-3} and 200 cm^{-3} and preshock magnetic field strengths $B_0 = 10^{-3}$ G and 10^{-4} G for the RD and SD zones, respectively. These field strengths may seem high compared to the typical interstellar magnetic field (10^{-6} to 10^{-5} G) or to the magnetic field of the WD at such distances. However, magnetohydrodynamic (MHD) simulations (Jun & Norman 1995) of SN remnants, characterized by a two-shock shell structure similar to the configuration considered here, show that Rayleigh-Taylor and Kelvin-Helmholtz instabilities may amplify ambient magnetic fields by 2 orders of magnitude or more. The signature of these instabilities is the clumpy nature of young SN remnants. The conspicuous clumpiness of the T Pyx shell, as seen in *Hubble Space Telescope* (*HST*) images (M. Shara, private communication), indicates that these instabilities caused turbulence in our case as well, thereby justifying the significantly amplified magnetic field strengths. The entire set of input parameters is given in Table 2, and the resulting line intensities relative to Hβ are given in Table 3. The observed line intensity–to–Hβ ratios are given in the second column. The corrected values, adopting $E_{B-V} = 0.08$, which is the value given by Williams (1982) for the ISM between T Pyx and Earth, appear in the third column. In the fourth column, the observed spectrum is corrected according to Selvelli et al. (1995), adopting $E_{B-V} = 0.31$ for

TABLE 3

COMPARISON OF MODEL CALCULATIONS WITH OBSERVATIONS

Line	Observed	Corrected ($E_{B-V} = 0.08$)	Corrected ($E_{B-V} = 0.31$)	RD	SD	RD + SD (1:3.6)
[O II] λ3727+	0.94	1.01	1.25	0.012	9.2	1.2
[O III] λ4363	0.13	0.14	0.15	0.19	0.55	0.24
He II λ4686	0.38	0.38	0.40	0.57	0.23	0.52
[O III] λ5007+	3.41	3.38	3.30	1.87	7.1	2.5
He I λ5876.....	0.08	0.07	0.06	8.3(−3)	0.36	0.05
[O I] λ6300+	...	...	...	2.(−5)	0.17	0.02
[N II] λ6548+	5.22	4.74	4.00	0.08	38.3	5.0
[S II] λ6717+	...	...	...	2.(−5)	0.8	0.10
Hβ (ergs cm^{-2} s^{-1}).....	...	...	...	8.7(−3)	3.6(−4)	...

the nebula. The RD and SD model results follow in the fifth and sixth columns, respectively, and the weighted average is given in the last column.

4.3. *The Radiation-dominated Zone*

In the RD case, the radiation of the hot star reaches the inner edge of the ionized slab, the very shock front edge. The adopted model is "matter bound," with a geometrical thickness $D_r \simeq 2.5 \times 10^{16}$ cm. This is roughly the thickness of the fraction of the recently ejected shell that lies between the reverse shock front and the edge of the old shell. Radiation-dominated models calculated in the "radiation-bound" case show nonnegligible [S II] and [O I] lines and, in general, line ratios that are different from the observed ones. The RD models were calculated for a range of parameters: V_s between 350 and 550 km s^{-1}, n_0 between 2000 and 5000 cm^{-3}, $B_0 > 10^{-4}$ G, $T_* > 10^5$ K, and U between 10^{-3} and 3×10^{-3}. Higher V_s values lead to very extended high-temperature postshock regions, so that the optical lines are emitted beyond the geometrical thickness of the slab; lower V_s values lead to very strong lines from the first and second ionization levels. The densities are related in particular to the [O II] λ3727+ doublet: higher densities would reduce too much the value of [O II]/Hβ, and the reverse would result from lower densities. An ionizing flux of $1–2 \times 10^{-3}$ and T_* about 2.5×10^5 K are consistent with the model of T Pyx. A higher flux would maintain the gas ionized at greater distances from the shock front, enhancing the neutral lines (e.g., [O I]).

Table 3 shows that for the RD model the He II/Hβ line ratio, which depends on the photon flux, is higher than 0.5. All the other line ratios are reduced significantly, particularly [N II]/Hβ, [O II]/Hβ, [S II]/Hβ, [O I]/Hβ, and He I/Hβ because the emitting gas at temperatures $<10^4$ K is cut out. Also, [O III]/Hβ is rather low relative to the observed value. In fact, shock velocities above 300 km s^{-1} maintain the gas at high temperatures (which correspond to higher ionization levels) in a extended postshock region (see Figure 2). Here strong X-ray emission results from bremsstrahlung.

4.4. *The Shock-dominated Zone*

Shock-dominated models were calculated with V_s between 200 and 300 km s^{-1}, n_0 between 100 and 300 cm^{-3}, and B_0 between 10^{-6} and 10^{-4} G, without limiting the extension of the emission region downstream. The thickness of the emitting zone, resulting in this case from the model, is found to be $\sim 5 \times 10^{16}$ cm. The velocities are assumed in agreement with the observations. Low preshock densities are adopted, as indicated by equation (8). As the Hβ absolute value increases with n^2 (where n represents the downstream density), and n, in turn, increases with V_s, the Hβ flux obtained for the SD model is lower than that corresponding to the RD model by a factor of more than 20. On the other hand, the SD spectrum shows enhanced low-ionization lines. As shown in Table 3, all the lines, except He II, are much stronger in the SD zone. The [O I] and [S II] line ratios to Hβ are low but nonnegligible.

The SD model contributes to [O II], [O III], and He I and, particularly, to [N II]. These line ratios to Hβ should be referred to the spectrum corrected by a lower reddening correction because they are emitted at the outer edge of the shell. The strong value of the [N II]/Hβ ratio explains why the luminosity of the T Pyx image in Hα + [N II] is strong in the extended shell, even if the Hα flux from the blast-wave postshock region is lower by some orders than that from the reverse postshock inner shell. The spectrum observed by Williams (1982) shows that the lines are blended strongly due to the relatively high FWHM.

4.5. *The Composite Spectrum versus Observations*

In conclusion, we consider a "matter-bound" RD model and a weighted average of the SD and RD models. The weight ratio (SD:RD), deduced phenomenologically so as to yield the best fit to observations, is 3.6:1.

In the last column of Table 3 the weighted model calculation results are compared with the observational data. The RD model contributes all the He II line flux and about half the [O III] flux; therefore, the calculated results for these line ratios should be compared with the observed values corrected by a higher obscuration. The calculated line intensities relative to Hβ are within a 30% error of the observed ones. In particular, the results of the calculations show average [O III] λ4363/Hβ and [O III] λ5007/Hβ higher and lower, respectively, than the observed counterparts. Considering, however, the number of parameters involved in the model and the possible observational error of the weak [O III] λ4363 line, which may be as high as 50% (Williams 1982), the fit is satisfactory.

In Figure 2 we show the schematic model of the T Pyx shell. On the left side, the reverse shock, propagating toward the WD, is reached by blackbody ionizing photons. The relatively high shock velocity leads to temperatures in excess of 10^7 K in the postshock region, and hence the gas remains fully ionized along the entire extent of the slab (2.6×10^{16} cm). At the outer edge of the postshock region, the temperature drops rapidly due to the high cooling rate, which is enhanced by the high density downstream. However, the cool region from which the low-ionization lines are emitted is cut off because the gaseous slab is "matter-bound." Besides the X-rays, which are strong due to high temperatures in the emitting gas, the integrated fluxes in the other frequency ranges (see Table 4) are high due to the high density. On the right side of Figure 2, the shock front of the outward propagating blast wave is shown. The temperatures and the densities in the postshock region are lower than in the RD postshock region, and therefore the fluxes in the different domains are lower (see Fig. 3). However, the extended region characterized by gas at temperatures lower than 10^4 K emits strong lines from low ionization levels. As the gas is maintained at $T_e \simeq 10^3$ K by diffuse (secondary) radiation, lines from fully recombined gas are low. Beyond 10^{16} cm away from the shock front,

TABLE 4

INTEGRATED FLUXES[a]

Type	Range (Hz)	RD Zone	SD Zone
Radio brem.....	10^7–10^{11}	1.6(−4)	1.1(−6)
IR dust	10^{10}–10^{14}	...	0.053
IR brem.....	10^{12}–10^{14}	0.32	2.0(−3)
Visible	3.10^{14}–10^{15}	0.34	1.9(−3)
UV	10^{15}–5.10^{15}	1.59	7.7(−3)
X-ray	$>10^{17}$	32.4	0.01

[a] In units of ergs cm^{-2} s^{-1}.

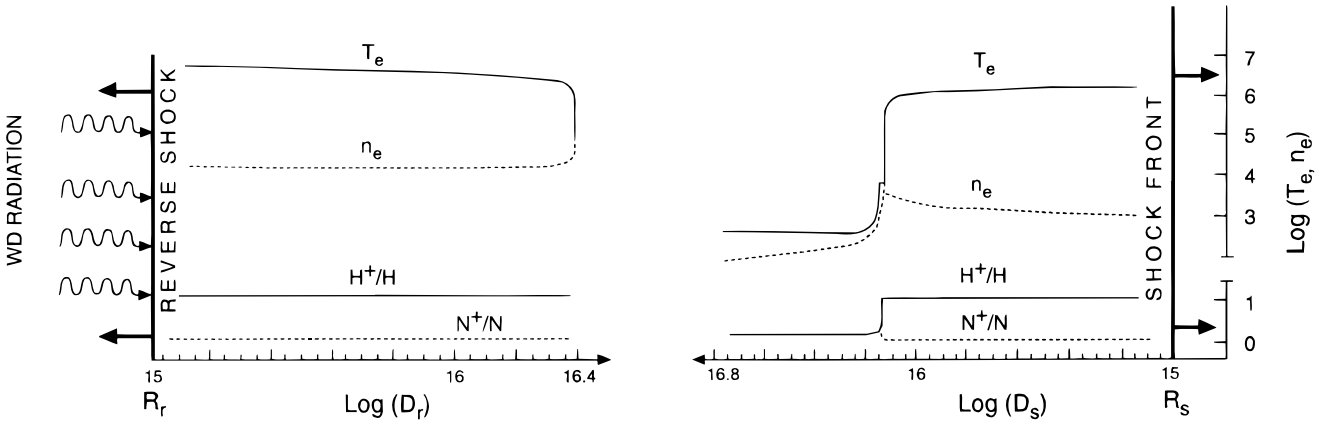

FIG. 2.—The model of T Pyx. Thick solid lines represent the shock fronts. The downstream distribution of the temperature (*solid lines*) and of the density (*dashed lines*) throughout the emitting gas are shown in the upper part of the figure. The fractional abundances of N^+/N (*dashed lines*) and of H^+/H (*solid lines*) downstream are given in the lower part of the figure. Distances are measured from each of the shock fronts on logarithmic scales.

$N^+/N > 0$ (the N^+/N fractional abundance is represented by the dashed lines at the bottom of Fig. 2) and N^+ recombines following H^+ due to charge exchange reactions.

Using equation (7), we obtain $R_r \simeq 5 \times 10^{16}$ cm. Thus, we have $R_r/R_s \sim 0.36$, in agreement with the observed angular dimensions of the two shells, $\theta \sim 2''$ and $\theta \sim 5''$. Accordingly, from equation (10), the contributions of the SD and RD zones should have been weighted roughly as 6:1. The discrepancy between this weight and the phenomenologically derived one is not severe, considering the relatively large widths of the emitting regions. The preshock gas densities in the two zones relate precisely as indicated by equation (8) and imply a low filling factor, of order 0.01 or less, as expected. The relative abundances of helium, carbon, and nitrogen are compatible with the requirement (9), assuming $\eta = 3$. The oxygen abundance is lower than that resulting from equation (9), indicating that some of the oxygen may be locked up in grains.

The absolute Hβ flux that should be measured at Earth can now be estimated from equation (10) using $R_r + D_r$ for the inner shell radius (rather than R_r), which yields $F_{H\beta} \approx 6 \times 10^{-14}$ ergs s^{-1} cm^{-2}, in good agreement with Williams's (1982) results, which yield $\sim 3 \times 10^{-14}$ ergs s^{-1} cm^{-2}, after correction for reddening with $E_{B-V} = 0.31$.

4.6. *The Continuum Spectrum*

The ratio of the weights of the RD to SD spectra, which is determined by the fit of the observed spectrum, determines the shape of the spectral energy distribution (SED) of the continuum. The results of our model are given in Figure 3—showing the continuum SED obtained for the SD and RD models and the flux emitted by the central source—together with observational results, calibrated for a distance of 2 kpc. The integrated fluxes in different frequency ranges, corresponding to Figure 3, for both RD and SD models are given in Table 4.

The radio-frequency continuum is stronger in the RD zone than in the SD zone; nevertheless, the radiation emitted in the RD zone is absorbed by the nebula beyond it, particularly the dense region behind the shock front (toward the observer), which is optically thick at low frequencies (Osterbrock 1974). Hence, only the (weaker) radio emission from the outer SD zone should be observable. The radio flux emitted by the SD zone is compatible to the observed one, as shown in Figure 3.

The moderate dust-to-gas ratio adopted for the SD model, $d/g = 5 \times 10^{-15}$, leads to a small infrared bump in the SED, which seems to be indicated by observations as well. Although the grains are heated by the gas entering the shock front, they are partly sputtered, and therefore the IR bump lacks the low-frequency range (see Contini, Orio, & Prialnik 1995). In the RD region, the dust grains are sputtered completely behind the shock front, and hence there is no (significant) contribution to the IR radiation from this region. We recall the low O/H relative abundance, indicating that oxygen could be included into dust grains and thus detracted from the gaseous phase. This is in agreement with the absence of [S II] lines in the observed spectrum, which indicates depletion of S; [S II] lines are emitted by gas in similar physical conditions as [N II] and [O II] for low densities and at roughly the same distance from the shock front. Sulphur, as well as oxygen, and particularly silicon, are included in silicates, which are the main constituents of dust grains.

The UV flux emitted by the shells that should be measured at Earth is estimated similarly to equation (10), to yield $F_{UV} \sim 10^{-11}$ ergs s^{-1} cm^{-2}. This is only about 4% of the UV flux detected by *IUE* (Selvelli et al. 1995). The UV luminosity is contributed by the central star, as was, indeed, inferred by Selvelli et al. and in agreement with the high effective temperature obtained for the WD (§ 2). The blackbody UV flux resulting from the WD luminosity is $\sim 1.1 \times 10^{-10}$ ergs s^{-1} cm^{-2}. The effect of this flux on the distant shell formed by the blast wave could, nevertheless, be neglected not only because of the larger distance of this shell from the source, but also because of absorption by the intervening dust. The reduced flux could not heat and ionize the gas to an extent comparable with the effect of the shock for $V_s > 200$ km s^{-1}. In fact, collisional ionization rates are correlated exponentially with the gas temperature and prevail strongly on radiation ionization rates for temperatures above 10^4 K. The UV lines, on the other hand, are emitted by the shocked gas. The strongest lines emitted in the RD zone are O VI λ1034, N V λ1240, C IV λ1550, He II λ1640, and C III λ1909. As this region is not continuous, but clumpy, the line strengths—correlated strongly with the

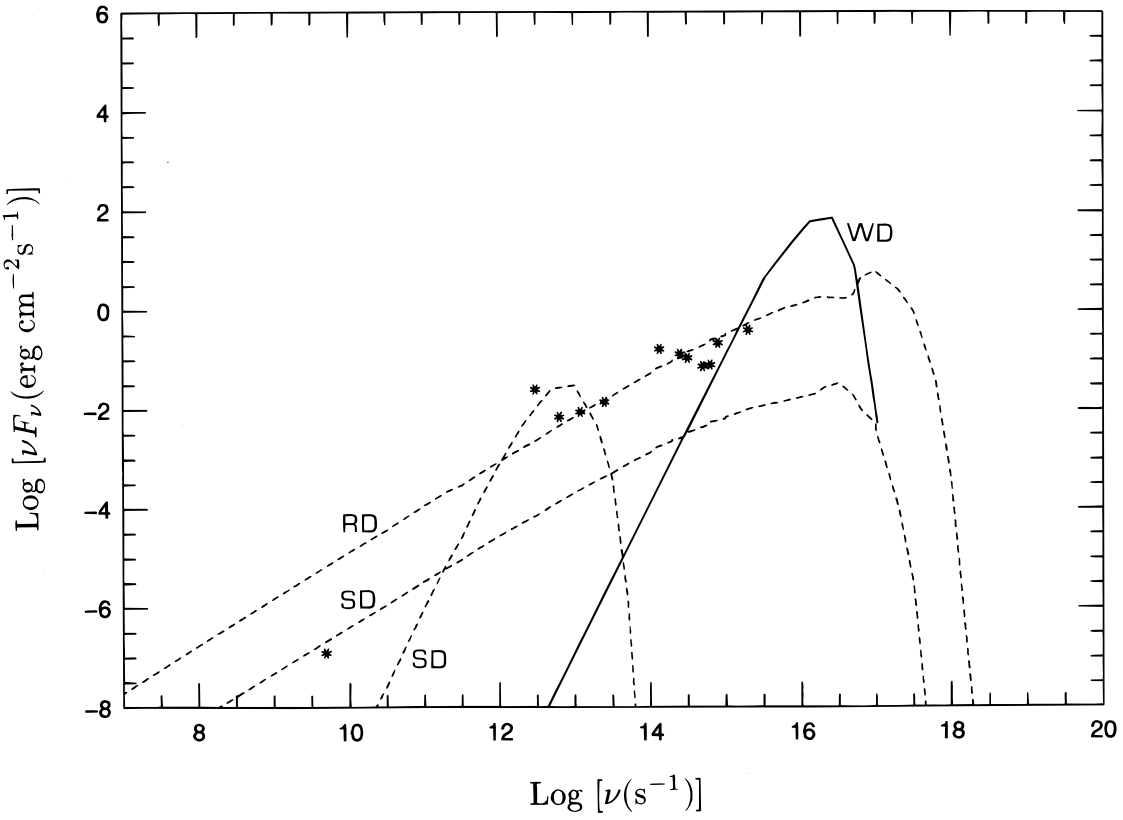

FIG. 3.—The SED of the continua in units of ergs cm^{-2} s^{-1} obtained for RD and SD models (*dashed lines*). The flux of the central source is represented by the solid line. Asterisks denote observational data: UV (λ1457) from Skody et al. 1991; *U*, *B*, and *V* from Bruch & Engel 1994; *B* and *V* from Skody et al. 1991; *K*, *J*, and *H* from Weight et al. 1994 and Harrison et al. 1993; low frequencies (IR and radio) from Weight et al. 1994.

density—are expected to show considerable variations, whereas the UV continuum emitted by the central source should be constant. The different sources for the continuum and the lines explain the *IUE* observations as analyzed by Selvelli et al. (1995), which show dramatic changes in the line intensities (C IV, He II, and N V), in marked contrast to the constancy of the continuum.

Finally, the rather hard X-rays (above 1.3 keV) are from the RD zone, where V_s and n_0 are higher. This result should be regarded as a prediction, as long as there are no observations in this range.

5. DISCUSSION AND CONCLUSIONS

We have presented a model for the observed nebula surrounding the RN T Pyx, which is compatible with the bulk of observational data that has accumulated during the quiescent period since the last outburst and with the general cyclic behavior of such a nova. The model, which simulates the physical conditions of an emitting gaseous slab under the coupled effects of photoionization and shocks, reproduces the observed spectral line intensity ratios and the absolute fluxes in different spectral ranges. The features of the central radiation source are obtained from an evolutionary model of nova outbursts, which reproduces most of the characteristics of T Pyx in eruption. The link between the ionization model and the shell model is based on dynamical considerations that combine both observed and inferred features of the ejecta. Thus, we show that shocks should, inevitably, play an important role. On the one hand, they are a direct consequence of the velocity distribution of the ejecta and of the short interoutburst period. On the other hand, they provide the only solution compatible with both the high expansion velocity of the ejected mass and the very slow expansion of the visible (emitting) shell(s).

The model involves two emitting regions besides the central star (which constitutes the main UV radiation source), both resulting from compressed gas behind a shock front. Different lines are emitted in these two regions, and, combined they account for the entire observed line spectrum. The shocks are produced by the collision between two extended shells, ejected at consecutive outbursts. As a result of the collision, a secondary blast wave propagates outward into the older ejecta, and a reflected (reverse) shock wave propagates back through the new ejecta. Although the emitting regions are associated with material ejected at different outbursts, they do not represent entire, separate, ejected shells, but rather dense, transient regions within the ejected shells. The model is shown schematically in Figure 4. The rate of expansion of the visible shells is determined by the velocity of the shock front, which may differ considerably from that of the gas. Thus, at the beginning, the shock velocity is much higher than the expansion velocity of the gas, which explains the large diameter of the bright shell 14 years after outburst. In time, the shock is decelerated, becoming a standing shock, which explains the imperceptible expansion of the bright shell during the last decade.

We cannot claim the model to be unique, in view of the many parameters involved, but we would like to stress that it is compatible with observations of widely different kinds pertaining to different evolutionary epochs: spectral line

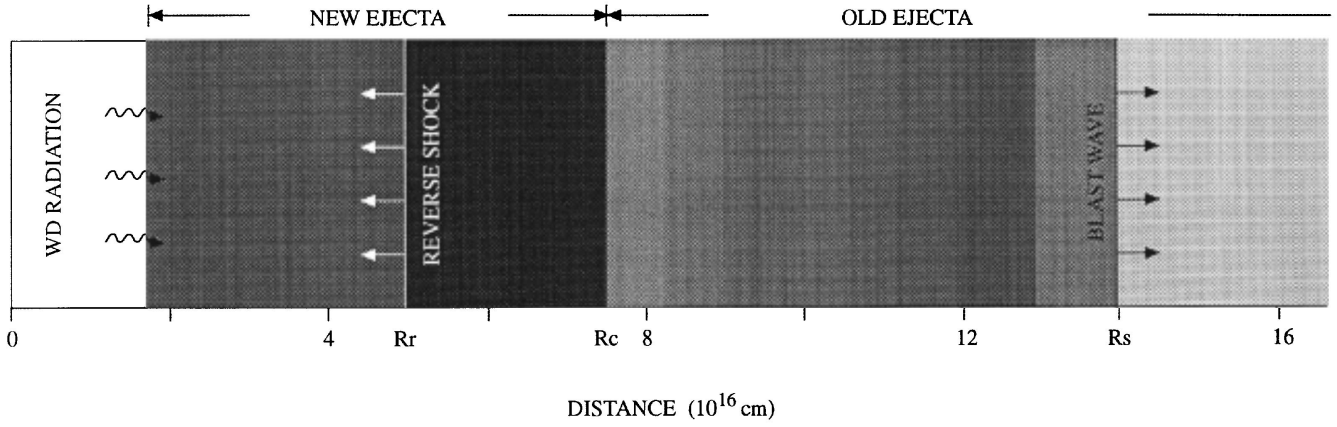

FIG. 4.—Schematic representation of the T Pyx nebula model, showing the two dense shells—emission sources—behind the shock fronts. Shading contrasts indicate relative densities.

intensity ratios, absolute fluxes in various ranges, shell locations, and gas velocities, as well as characteristics of the eruption, which bear on observed features in quiescence. The predictions of this model are open to testing by observations during the imminent next outburst of T Pyx.

In recent years, shocks have been invoked to explain the characteristics of the ejecta in several recurrent and symbiotic novae, e.g., RS Ophiuchi (Contini et al. 1995; Shore et al. 1996) and HM Sagittae (Formiggini, Contini, & Leibowitz 1995). Nova T Pyx provides yet another example for the successful explanation of the characteristics of these objects by shock models. We should add that very different circumstances are encountered in the different cases involving shocks, which goes to prove the general importance of this mechanism for the emission features of nova shells.

We wish to thank Mike Shara for illuminating discussions about this peculiar nova, which inspired this work, and Pierluigi Selvelli for providing UV spectra prior to publication.

REFERENCES

Andreä, J., Dreschsel, H., Snijders, M. A. J., & Cassatella, A. 1991, A&A, 244, 111
Bruch, A., & Engel, A. 1994, A&A, 104, 79
Catchpole, R. M. 1969, MNRAS, 142, 119
Chevalier, R. A. 1982, ApJ, 258, 790
Contini, M., & Aldrovandi, S. M. V. 1983, A&A, 127, 15
Contini, M., Orio, M., & Prialnik, D. 1995, MNRAS, 275, 195
Duerbeck, H. W. 1987, ESO Messenger, No. 50, 8
Duerbeck, H. W., & Seitter, W. C. 1990, in Physics of Classical Novae, ed. A. Cassatella & R. Viotti (Berlin: Springer-Verlag), 425
Formiggini, L., Contini, M., & Leibowitz, E. 1995, MNRAS, 277, 1071
Gull, S. F. 1973, MNRAS, 161, 47
———. 1975, MNRAS, 171, 263
Harrison, T. E., & Gehrz, R. D. 1994, AJ, 108, 1899
Harrison, T. E., Johnson, J. J., & Spyromilio, J. 1993, AJ, 105, 320
Jun, B.-I., & Norman, M. L. 1995, in Shocks in Astrophysics, ed. T. J. Miller & A. C. Raga (Dordrecht: Kluwer), 267
Kato, M. 1990, ApJ, 362, L17
Osterbrock, D. E. 1974, Astrophysics of Gaseous Nebulae (San Francisco: Freeman)
Ostriker, J. P., & McKee, C. F. 1988, Rev. Mod. Phys., 60, 1
Payne-Gaposhkin, C. 1957, The Galactic Novae (Amsterdam: North Holland)
Prialnik, D. 1986, ApJ, 310, 222
Prialnik, D., & Kovetz, A. 1995, ApJ, 445, 789
Seaquist, E. R., & Taylor, A. R. 1990, ApJ, 349, 313
Sedov, L. I. 1959, Similarlity and Dimensional Methods in Mechanics (New York: Academic Press)
Seitter, W. C. 1986, in RS Ophiuchi and the Recurrent Nova Phenomenon, ed. M. F. Bode (Amsterdam: VNU), 63
Selvelli, P. L., Gilmozzi, R., & Cassatella, A. 1995, in Cataclysmic Variables, ed. A. Bianchini, M. Della Valle, & M. Orio (Dordrecht: Kluwer), 182
Shara, M. M., Moffat, A. F. J., Williams, R. E., & Cohen, J. G. 1989, ApJ, 337, 720
Shore, S. N., Kenyon, S. J., Starrfield, S., & Sonneborn, G. 1996, ApJ, 456, 717
Skody, P. 1994, AJ, 108, 639
Skody, P., Stablein, C., Mattei, J. A., & Waagen, E. O. 1991, ApJS, 76, 359
Snijders, M. A. J., Batt, T. J., Seaton, M. J., Blades, J. C., & Morton, D. C. 1984, MNRAS, 211, 7P
Starrfield, S., Sparks, W. M., & Truran, J. W. 1985, ApJ, 291, 136
Viegas, S. M., & Contini, M. 1994, ApJ, 428, 113
Warner, B. 1995, Cataclysmic Variable Stars (Cambridge: Cambridge Univ. Press)
Webbink, R. F., Livio, M., Truran, J. W., & Orio, M. 1987, ApJ, 314, 653
Weight, A., Evans, A., Naylor, T., Wood, J. H., & Bode, M. F. 1994, MNRAS, 266, 761
Williams, G. 1983, ApJS, 53, 523
Wiiliams, R. E. 1982, ApJ, 261, 170
———. 1989, AJ, 97, 1752